CELL CYCLE
2020, VOL. 19, NO. 22, 3042–3053
https://doi.org/10.1080/15384101.2020.1829800

Taylor & Francis
Taylor & Francis Group

RESEARCH PAPER

Gypenosides improves nonalcoholic fatty liver disease induced by high-fat diet induced through regulating LPS/TLR4 signaling pathway

Shuhua Shen[a], Kungen Wang[b], Yihui Zhi[b], Wei Shen[c], and Liquan Huang[b]

[a]Disease Prevention and Health Management Center, The First Affiliated Hospital of Zhejiang University of Traditional Chinese Medicine, Hangzhou, Zhejiang Province, China; [b]Department of Traditional Chinese Internal Medicine, The First Affiliated Hospital of Zhejiang University of Traditional Chinese Medicine, Hangzhou, Zhejiang Province, China; [c]Center of Hospital-made Preparations, The First Affiliated Hospital of Zhejiang University of Traditional Chinese Medicine, Hangzhou, Zhejiang Province, China

ABSTRACT

Background The contents of lipopolysaccharide (LPS) and Toll-like receptor 4 (TLR4) are significantly increased during the progression of nonalcoholic fatty liver disease (NAFLD). The study investigated the role of the LPS/TLR4 signaling pathway in improving gypenosides (Gyp) on NAFLD. Methods NAFLD model were established in rats and treated by Gyp. Pathological changes of liver tissues were observed by Hematoxylin and Eosin (HE) staining. Lipid metabolism and insulin resistance were measured. Expressions of inflammatory factors and protein of LPS/TLR4 downstream pathway were detected by qRT-PCR and Western blotting. THLE-2 cells were treated by free-fatty acid (FFA), Gyp, and LPS, and then transfected with TLR4. Next, cell viability was detected by MTT. Lipid droplet deposition and Triglyceride (TG) content were determined by Oil Red O staining and ELISA. Results Gyp protected fatty liver tissues in NAFLD model, and significantly reversed cholesterol increased by high-fat diet. Moreover, Gyp increased SOD content and decreased the contents of AST, ALT, MDA, HSI, FBG, FINS, HOMA-IR, IL-1β, and TNF-α, and promoted the expressions of TLR4, LPS, MyD88, p-IκBα, and reduced the expressions of p-p65 and IκBα in the NAFLD model. Gyp treatment significantly reduced lipid droplet deposition, increased TG content and MyD88, p-IκBα, p-p65 in FFA-induced liver cells, but LPS and TLR4 greatly reversed improvement of FFA by Gyp. Conclusion Gypenosides could improve liver function, lipid metabolism, insulin resistance, and levels of inflammatory factors in NAFLD model by regulating LPS/TLR4 signaling pathway *in vitro* and *in vivo*.

ARTICLE HISTORY
Received 29 February 2020
Revised 10 September 2020
Accepted
16 September 2020

KEYWORDS
Gypenosides; nonalcoholic fatty liver disease; lipid metabolism; insulin resistance; LPS/TLR4 signaling pathway

Introduction

Nonalcoholic fatty liver disease (NAFLD) is a clinicopathologic syndrome characterized by steatosis and fat accumulation in liver parenchymal cells, and its progression is susceptible to obesity and diabetes [1,2]. Studies have shown that high-fat diet is closely related to the onset of NAFLD, and the treatment of fatty liver complicated with hyperlipidemia still faces great challenges, because some lipid-lowering drugs focus more on liver metabolism, and once liver lipid metabolism is impaired, liver function will be impaired, causing difficulties in lipid-lowering in NAFLD patients [3,4]. Therefore, the exploration of effective treatment for NAFLD is the key to current research.

Toll-like receptor 4 (TLR4) is an important member of the TLRs family. According to studies, TLR4 is involved in a variety of liver diseases and plays a key role in the pathogenesis of inflammation [5,6]. Both DAMPs released by damaged and necrotic cells and fatty acids accumulated in the liver can activate TLR4 [7], and TLR4 is expressed in both macrophages and neutrophils [8,9]. In addition, research has confirmed that TLR4 is a key recognition pattern receptor for LPS and plays a vital role in linking the innate immune system and metabolic syndrome [10]. Therefore, in this study, in order to explore the new treatment mechanism of NAFLD, we tested the LPS/TLR4 signaling pathway related factors.

The pathogenesis of NAFLD is complex and has not yet been clarified. At present, it is believed that it may be related to factors such as endotoxemia and inflammatory response [11–13]. LPS is an endotoxin in the cell wall, which is currently considered to be one of the main factors of the

CONTACT Shuhua Shen shenshuhua_sh@163.com

pathogenesis and progress of NAFLD. It enters the blood circulation, through which it is transported to the target tissue and recognized by immune cells. Then inflammatory signaling pathway was activated, and pro-inflammatory factors were secreted, the body therefore entered a state of chronic low-grade inflammation and metabolic abnormality was induced [14,15].

With the continuous progress of traditional Chinese medicine research, Chinese medicine had shown its therapeutic effects and fewer side effects in clinical practice [16], suggesting it may also has the potential in effective lipid-lowering and liver-protecting. Studies found that Gypenosides (Gyp) has anti-tumorous property, and could enhance immune system, lower blood lipid, and inhibit platelet aggregation [17,18]. Moreover, Gyp could inhibit hepatic steatosis in rats with NAFLD [18]. However, the role of its LPS/TLR4 signaling pathway in improving NAFLD was still unclear. Therefore, in this study, we established a high-fat liver model in rats and cells to explore the role and mechanism of LPS/TLR4 signaling pathway in improving NAFLD of Gyp.

Materials and methods

Ethics statement

The animal experiments were approved by the Animal Ethics Committee of The First Affiliated Hospital of Zhejiang University of Traditional Chinese Medicine (FAH20180523). The animal experiments were conducted strictly in accordance with the guidelines of the National Institutes of Health (USA).

Establishment and treatment of model rats

A total 32 of 6-week-old male Wistar rats (200 ± 20 g) were obtained from SLAC Laboratory Animal Technology Co., Shanghai, China. The rats were raised at the temperature of 20–26°C in 40–70% humidity under a 12 light/12 dark cycle and fed with a normal diet. The rats were randomly assigned into 4 groups (n = 8) as follows: Control group, Model group, Model + Gyp group, and Gyp group.

For control group, the rats were only fed with normal basal food.

For model group, NAFLD was established in rats as a rat model. Briefly, the rats were fed with a high-fat diet (mainly formulated from 88% basal feed, 10% lard, and 2% cholesterol) for 12 weeks.

For Model + Gyp group, after the 12 th week of the high-fat diet for established NAFLD model, rats in the model group were randomly separated into the model group, Model + Gyp group. The rats in Model + Gyp group were treated with 11.49 mg/kg weight/d Gyp (number: ZL150307100; specification: 98%; yield: 60: 1, Nanjing Zelang Pharmaceutical Technology Co., Ltd.) by intragastric gavage administration for 12 weeks.

After all rats in each group were fed for 12 weeks, the liver weight and body weight of rats were measured to calculate liver weight/body weight ratio, which is alternatively known as the hepatic steatosis index (HSI). Fasting insulin (FINS) level was detected by I–insulin radioimmunoassay kit. Insulin resistance (HOMA-IR) of the rats was evaluated according to HOMA-IR = FINS × FBG/22.5.

Hematoxylin and eosin (HE) staining

The liver tissues were subjected to HE staining. Briefly, after the tissues were fixed in formaldehyde for 24 h, 5-μm tissue sections were prepared after alcohol dehydration, made transparent by and paraffin-embedded, and then sections were stained with hematoxylin (G1120, Solarbio, China) for 20 min. Next, the sections were immersed in the acidified solution for 1 min to remove the blue from the cytoplasm, and stained by eosin for 15 min. After the tissue sections were dehydrated and became transparent, the membrane was sealed with neutral gum, and the pathological changes of the liver tissues were observed under an optical microscope (CKX31, Olympus, Japan).

Determination of serum enzymes, fasting blood glucose (FBG), and blood lipids

The blood collected from the rat inferior vena cava was centrifuged at 3000 × g for 15 min at room

temperature to take the upper layer of serum was taken. A fully automatic biochemical detection analyzer (SYSMEX CHEMIX-180) was used to detect serum enzymes including alanine aminotransferase (ALT), aspartate aminotransferase (AST), and FBG levels to assess liver damage. Moreover, By measuring the content of serum TC and triglyceride (TG) in rats, the blood lipid level of rats was evaluated. Briefly, 50 mg liver tissues were collected and washed with PBS twice, then added with 20 μl/mg of lysate and centrifuged at 2000 × g for 5 min. Then supernatant was taken and analyzed by a fully automatic biochemical analyzer.

Determination of levels of malondialdelyde (MDA) and superoxide dismutase (SOD)

The levels of SOD and MDA in serum from each group of rats were measured according to the instruction of the SOD assay kit (19160, Sigma-Aldrich, USA) and MDA assay kit (MAK085, Sigma-Aldrich, USA), respectively. All reagents were prepared and added to the cells in sequence according to the requirements of the SOD and MDA assay kit. The cell supernatant was then put in a water bath pot at 37°C for 10 min. Next, the colorant was added to the cell supernatant and maintained at room temperature for 10 min, and the absorbance was determined at 550 nm and 532 nm by a microplate reader.

Cell treatment

THLE-2 cells were purchased from American Type Culture Collection (CRL-2706, ATCC, Rockville, MD, USA). Dulbecco's modified Eagle's medium (DMEM; C11885500BT, Guangzhou saiguo biotech Co., Ltd, China) containing 10% fetal bovine serum (FBS; 10437010, Gbico) was used to culture THLE-2 cell lines with 5% CO_2 at 37°C in a humid incubator. THLE-2 cells were treated with different concentrations (0 μmol/L, 10 μmol/L, 20 μmol/L, 40 μmol/L, 80 μmol/L, 160 μmol/L, and 320 μmol/L) of Gyp. In addition, after the THLE-2 cells were treated with 1 mM free-fatty acid (FFA) (Oleic: palmitic acid = 2:1) for 24 h, the 40 μmol/L Gyp was used to treat the cells for 24 h at 37°C. 50 ng/ml lipopolysaccharide (LPS) was used to stimulate the FFA-induced cells for 24 h at 37°C.

Transfection

To investigate the effects of TLR4 on FFA-induced cells, TLR4 sequence was synthesized by Guangzhou RiboBio Co., Ltd. and cloned into the pcDNA3.1 vector (cat. no. V79020; Thermo Fisher Scientific, Inc.). Then the treated vector was transfected into the cells (3×10^5 cells) using Lipofectamine™ 2000 transfection reagent (11668019, Invitrogen, Carlsbad, California, USA). For comparison, untransfected cells served as blank controls, whereas those transfected with empty vector served as negative controls (NC).

Cell viability detection

Methylthiazolyldiphenyl-tetrazo lium bromide (MTT) kit (C0009, Beyotime Biotechnology, China) was used to detect the viability of the cells. The cells were inoculated into the 96-well plate (2×10^3 cell/well) in 95% humidified environment with 5% CO_2 at 37°C. After treatment, the cells were added with the test compound at an appropriate concentration, and the culture was continued for an appropriate time. After cell culture, the supernatant was carefully removed, and the cells were added with 90 μL fresh culture medium and further incubated with 10 μL MTT solution for 4 h. Then the supernatant was removed, added with 110 μL formazan solution, and shaken on a shaker at low speed for 10 min to fully dissolve the crystals. The absorbance of each well was measured at 490 nm by a microplate reader (BMG Labtech, Germany).

Oil Red O staining

To investigate the effect of Gyp on FFA-processed cell adipogenesis, the cells were stained by Oil Red O detection kit (G1262, Solarbio, China). The cell culture medium was removed, and the cells were washed twice with PBS, and fixed with ORO fixative for 20–30 min. The fixative was discarded and

the cells were washed twice with distilled water. The cells were stained by the freshly prepared ORO and incubated for 10–20 min. Then, mayer hematoxylin staining solution was added and to counterstain the nucleus for 1–2 min. Next the dye solution was discarded and the cells were washed with water twice to five times. Distilled water was added to cover the cells, which were then observed under a microscope. Finally, an optical microscope (CKX31, Olympus, Japan) was used to observe the cells adipogenesis.

Determination of triglyceride (TG) content in cells

The experiment was performed according to the instructions of glycerol tri-cooled quantification kit (K622-100, BioVision, USA). Specifically, a standard curve was prepared, and cell lysate was added to the model group and control group cells. Half of each group of cells was taken for determining the protein concentration, while the other half were heated in an 80°C water bath for 3 min, and subsequently the cell supernatant was tested for TG content. Then the extracted cell supernatant was added to a standard well, incubated at room temperature for 60 min in the dark, and the absorbance of each well was measured at a wavelength of 570 mn by microplate reader. The absorbance value was subtracted without the TG standard from all sample readings and a standard curve was plotted. The sample reading was integrated into the standard curve to calculate the triglyceride concentration (fimol/ml), and divided according to the protein concentration (mg/ml) of the corresponding samples as the final result in the comparison of intracellular glycerol between different groups.

Enzyme-linked immunosorbent assay (ELISA) for lipopolysaccharide (LPS) activity

THLE-2 cells were treated with FFA and Gyp, seeded (2×10^3/well) into 96-well plates, and incubated overnight. The cell supernatants were collected for measuring LPS viability by LPS ELISA kits (CSB-E09945h, Wuhan Huamei Biological Engineering Co. LTD, Hubei, China).

Quantitative reverse transcription-polymerase chain reaction (qRT-PCR)

Total RNAs were extracted from tissues or cells by Trizol reagent (12183555, Thermo Fisher Scientific, USA), and the RNA concentration was measured by NanoDrop™ One/OneC micro-uv-visible spectrophotometer (ND-ONEC-W, Thermo Scientific™, USA). The RNA concentration at 500 ng/μL, it was used for subsequent experiments. Then, the RNAs was reverse-transcribed into cDNA by PrimeScript RT kit (RR037A, Takara, China). The mRNA expressions were determined by using a SuperScript™ III Platinum™ SYBR™ Green One-Step qRT-PCR Kit (11736059, Thermo Fisher Scientific, USA). GAPDH served as internal reference. PCR amplification system was composed of 1 μl distilled water, 3 μl cDNA, 5 μl DNA polymerase, and 1 μl Primer. The ABI7500 system (Applied Biosystems) was used in a qRT-PCR reaction, and $2^{-\Delta\Delta CT}$ method was used to calculate the multiple changes of relative mRNA expression levels [19, 20]. The PCR cycle system was set as follows: at 95°C for 10 min, at 95°C for 15 s, at 72°C for 15 s, for a total of 40 cycles. All primer sequences of qRT-PCR in this study were listed in Table 1.

Western blotting

RIPA buffer (P0013B, Beyotime Biotechnology, China) was used to lyse the total proteins in tissues, cells and cytoplasm and nucleus of cells. BCA kit (P0012S, Beyotime Biotechnology, China) was used to measure the protein concentration. The proteins were separated by electrophoresison 15%

Table 1. Primers used in real-time PCR analysis.

Gene	Primer sequence	Species
IL-1β	Forward: 5 -ATAAGCCCACTCTACACCT-3 reverse: 5 -ATTGGCCCTGAAAGGAGAGA-3′	rat
TNF-α	Forward: 5 -TGCTCCTCACCCACACCAT-3 reverse: 5 -GCCCAGACTCGGCAAAGTC-3′	rat
TLR4	Forward: 5 -GAATGCCTAAGGTTGGCACTCTC-3 reverse: 5 -CTCAGGCAGGAAAGGAACAATG-3′	rat
β-actin	Forward: 5 -CTGGAGAAGAGCTATGAG-3 reverse: 5 -ATGATGGAATTGAATGTAGTT-3′	rat

Abbreviations: IL-1β, Interleukin-1β; TNF-α, Tumor necrosis factor-α; TLR4, Toll-like receptor 4

Table 2. Weight data of rats.

	Control	Model	Model+Gyp	Gyp
Body weight (g)	522.40 ± 38.56	523.04 ± 36.78	522.22 ± 32.17	528.91 ± 42.96
Liver weight (g)	14.47 ± 3.03	20.86 ± 4.35**	16.43 ± 3.11$^{\wedge\wedge\#}$	14.38 ± 3.16

**$P < 0.01$ vs. Control; $^{\wedge\wedge}P < 0.01$ vs. Model; $^{\#}P < 0.05$ vs. Gyp

dodecyl sulfate sodium salt-Polyacrylamide gel electrophoresis (P0508S, Beyotime Biotechnology, China), and then moved to polyvinylidene fluoride membranes (FFP24, Beyotime Biotechnology, China), which were sealed by 5% milk at 25°C for 1 h. Then primary antibodies (MyD88 (ab2064, 35KD, Abcam, USA), p-IκBα(#2859, 40KD, CST, USA), IκBα (#4814, 39KD, CST, USA), p-p65(ab86299, 60KD, Abcam, USA), TLR4 (ab13556, 100kD, Abcam, USA), p65 (ab16502,64KD, Abcam, USA) and β-actin (ab8226,42kD) were used to incubate the proteins at 4°C overnight, The membranes were further incubated with the secondary antibody (Protein tech, USA) for 2 h and washed by PBS for three times. ECL kit (D3308, Beyotime Biotechnology, China) was used to develop the protein bands, which were scanned by a super sensitive multi-functional imager (Amersham Imager 600, General Electric Company, USA).

Statistical analysis

SPSS 18.0 (Chicago, USA) was used to analyze the data, which were shown as mean ± standard deviation. Group differences were measured by ANOVA followed by Tukey post-hoc test, and *t* test was used to compare the difference between two groups of data. Each treatment was carried out in triplicate. $P< 0.05$ was considered as statistically significant.

Results

Effect of Gypenosides on liver tissue damage and biochemical indicators in NAFLD rat model

Nonalcoholic fatty liver disease (NAFLD) rat model was established, and liver tissues of the model rats were used for pathological observation. As shown in Figure 1(a), cytoplasmic vacuoles and lipid droplets were observed in the liver cells of the model group of rats, indicating that the liver cells were severely necrotic. However, these liver pathological changes were significantly improved by Gyp. The results showed that Gyp protected fatty liver caused by a high-fat diet. Next, the effect of Gyp on blood lipids and cholesterol in model rats was examined by detecting the levels of TC and TG. As shown in Figure 1(b and c), Gyp significantly reversed the increased levels of TC and TG in model rats ($P< 0.05$, $P< 0.001$). Then, the effects of Gyp on the expression levels of AST and ALT in the model rats were detected, and the results showed that Gyp significantly reduced the levels of AST and ALT caused by high-fat diet in the rats (Figure 1(d and e), $P< 0.05$, $P< 0.01$). Furthermore, the oxidative stress indicators of the model rats induced a decrease in SOD activity and an increase in MDA level in the rats fed with a high-fat diet ($P< 0.001$). Then we detected the effect of Gyp on the oxidative stress indicators of the model rats. High-fat diet decrease SOD, and Gyp significantly reduced the increase in MDA caused by high-fat diet (figure 1(f and g), $P< 0.01$). In addition, Gyp greatly reduced the levels of HIS, FBG, FINS and HOMA-IR in model rats increased by high-fat diet (Figure 2 (a-d), $P< 0.05$, $P< 0.01$, $P< 0.001$).

Effect of Gypenosides on inflammatory factor and LPS/TLR4 downstream pathway in NAFLD rat model

Furthermore, the inflammatory factor was detected in Gyp-treated NAFLD rats by qRT-PCR. The results showed that the expressions of IL-1β, TNF-α, and TLR4 were increased in NAFLD rat, which was reversed by Gyp (Figure 2(e), $P< 0.01$). In addition, the effect of Gyp on LPS/TLR4 downstream pathway on the NAFLD rat model was explored by detecting and comparing the expressions of MyD88, p-IκBα, κBα, TLR4 and p-p65 and p65 by Western blotting. The results showed that Gyp significantly decreased

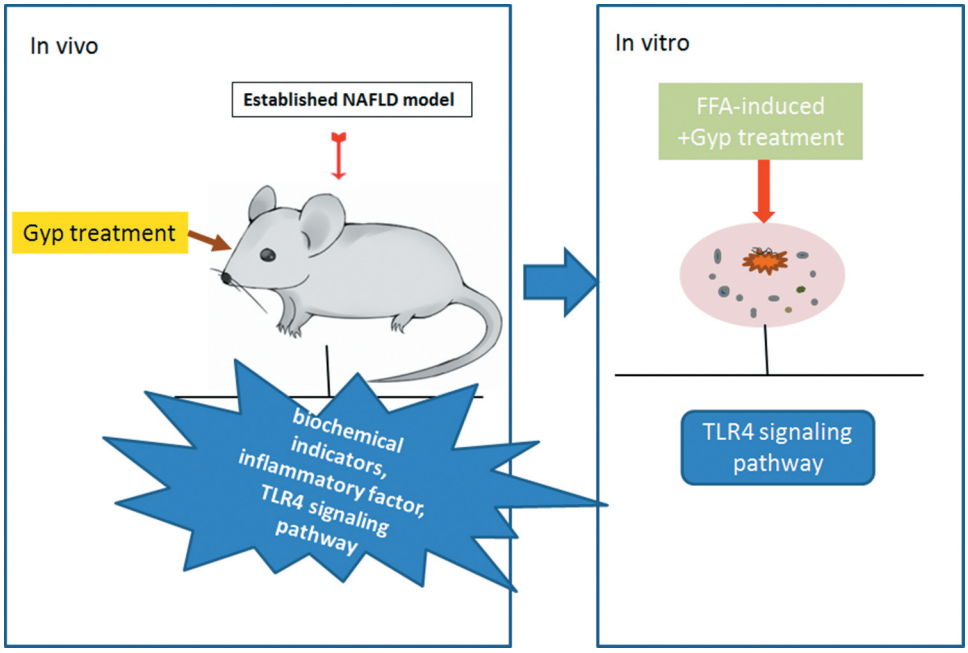

Figure 1. Effect of Gypenosides on liver tissue damage and biochemical indicators in NAFLD rat model. (a) Pathological changes of liver tissue were observed by hematoxylin and eosin (HE) staining in NAFLD rat model that treated with Gyp. (b) The scores were counted according to HE staining. (c) Serum total cholesterol level was detected by serum total cholesterol kit. (d) Triglyceride level was measured by triglyceride kit. (e) Aminotransferase (AST) level was detected by AST kit. (f) Alanine transaminase (ALT) level was detected by ALT kit. (g) Superoxide dismutase (SOD) level was detected by SOD kit. (h) Malondialdehyde (MDA) level was detected by MDA kit. n = 3, $^{*}P < 0.05$, $^{**}P < 0.01$, $^{***}P < 0.001$, vs. Control; $^{\wedge}P < 0.05$, $^{\wedge\wedge}P < 0.01$, $^{\wedge\wedge\wedge}P < 0.001$, vs. Model; $^{\#}P < 0.05$, $^{\#\#}P < 0.01$, $^{\#\#\#}P < 0.001$, vs. Control.

the levels of LPS, MyD88, TLR4, p-IκBα, p-p65, and IκBα caused by high-fat diet (figure 2(f-j), $P< 0.001$). QRT-PCR detected the expression of iNOS gene, and the results showed that Gyp significantly reduced the increase of iNOS caused by high-fat diet in liver tissue (Figure 2(k), $P< 0.001$).

The effect of Gypenosides on FFA-induced adipogenesis in THLE-2 cells and the effect on LPS/TLR4 downstream pathways in THLE-2 cells

The THLE-2 cells were treated with FFA to establish the high-fat model. The cells were cultured for 48 h with different concentrations of Gyp, and the cell viability was measured by MTT assay. As shown in Figure 3(a), high concentration of Gyp was slightly toxic to THLE-2 cells ($P< 0.05$). After the cells were cultured in an adipogenic medium, the cells were stained with Oil Red O, and we found that 40-μM Gyp treatment significantly reduced FFA-induced cell lipid deposition (Figure 3(b and c)). Meanwhile, the cell TG was detected by kit, and the results showed that Gyp treatment significantly reduced the increase of TG content in FFA-induced steatotic liver cells (Figure 3(d), $P< 0.01$). QRT-PCR detected iNOS gene expression, the results showed that Gyp treatment can significantly reduce the increase of iNOS in steatosis hepatocytes induced by FFA (Figure 3(e), $P< 0.001$). In addition, the effect of Gyp on LPS/TLR4 downstream pathway on the NAFLD rat model was explored, and the expressions of MyD88, p-IκBα, κBα, and p-p65 and p65 were detected by Western blotting. The data demonstrated that Gyp significantly decreased the levels of TLR4, LPS, MyD88, p-IκBα, and p-p65 caused by high-fat diet, and increased IκBα level (Figure 3(f-i), $P< 0.05$, $P< 0.01$, $P< 0.001$). Moreover, Western blotting was used to detect the expression of p65 in cytoplasm and

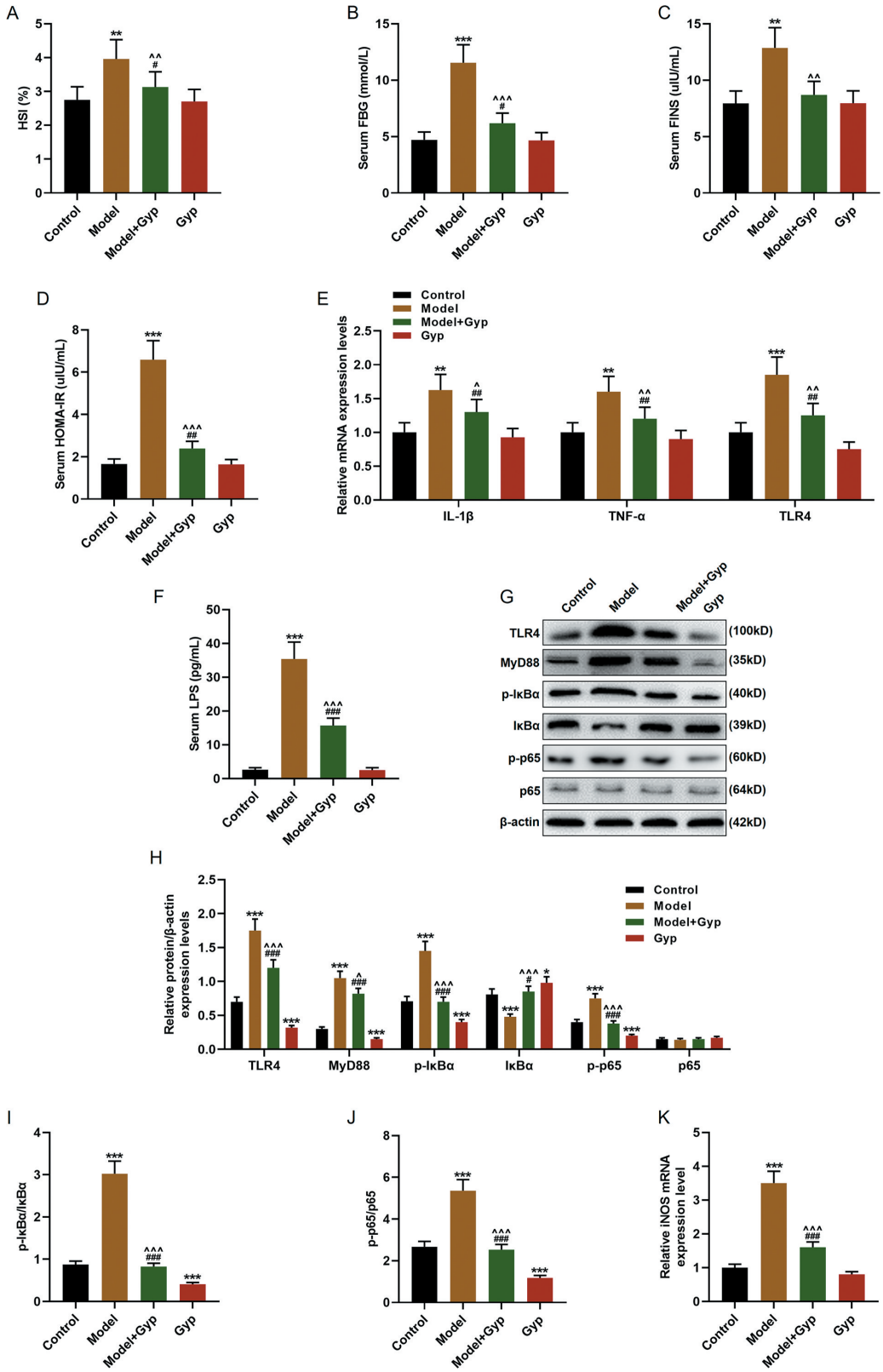

Figure 2. Effect of Gypenosides on biochemical indicators and inflammatory factor and LPS/TLR4 downstream pathway in NAFLD rat model (a) hepatic steatosis index (HSI) of rats was evaluated. (b) Fasting blood glucose (FBG) of rats was measured. (c) Fasting insulin (FINS) of rats was detected. (d) Insulin resistance (HOMA-IR) of rats was evaluated. (e) The expressions of IL-1β, TNF-α, and TLR4 were detected by qRT-PCR. (f) Serum LPS concentration was detected by ELISA kits. (G, H, I and J) The expressions of TLR4, MyD88, p-IκBα, κBα and p-p65 and p65 were detected by Western blotting. (k) QRT-PCR was used to detect the iNOS expression in liver tissue. $n = 3$, $^{*}P < 0.05$, $^{**}P < 0.01$, $^{***}P < 0.001$, vs. Control; $^{\wedge}P < 0.05$, $^{\wedge\wedge}P < 0.01$, $^{\wedge\wedge\wedge}P < 0.001$, vs. Model; $^{\#}P < 0.05$, $^{\#\#}P < 0.01$, $^{\#\#\#}P < 0.001$, vs. Control.

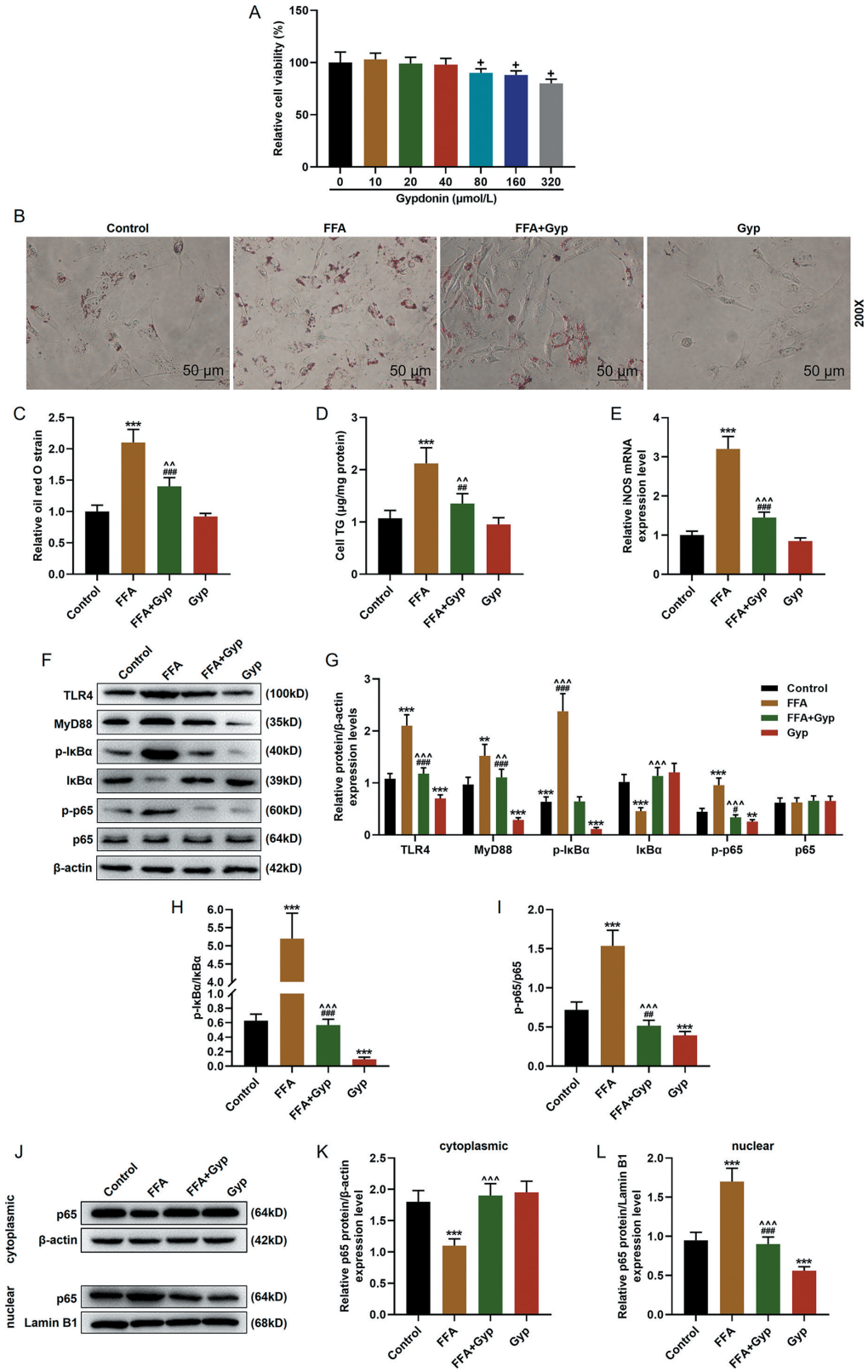

Figure 3. The effect of Gypenosides on FFA-induced adipogenesis in THLE-2 cells and the effect on LPS/TLR4 downstream pathways in THLE-2 cells (a) MTT was used to detect the viability of THLE-2 cell treated with different concentrations of Gyp (10 μmol/L, 20 μmol/L, 40 μmol/L, 80 μmol/L, 160 μmol/L, and 320 μmol/L,). (b and c) Oil Red O staining was used to detect lipid droplet deposition of FFA-induced THLE-2 cell that treated with 40 μmol/L Gyp. (d) Kit used to detect triglyceride (TG) content in cells. (e) The iNOS expression was detected by qRT-PCR in cells. (F, G, H and I) The expression levels of TLR4, MyD88, p-IκBα, κBα, and p-p65 and p65 were detected by Western blotting. (J, K, and L) The p65 expression in cytoplasm and nucleus were detected by Western blotting. $n = 3$, $^{+}P < 0.05$, $^{++}P < 0.01$, $^{+++}P < 0.001$, vs. 0; $^{*}P < 0.05$, $^{**}P < 0.01$, $^{***}P < 0.001$, vs. Control; $^{\wedge}P < 0.05$, $^{\wedge\wedge}P < 0.01$, $^{\wedge\wedge\wedge}P < 0.001$, vs. FFA; $^{\#}P < 0.05$, $^{\#\#}P < 0.01$, $^{\#\#\#}P < 0.001$, vs. Gyp; $^{\&}P < 0.05$, $^{\&\&}P < 0.01$, $^{\&\&\&}P < 0.001$, vs. FFA+Gyp+NC.

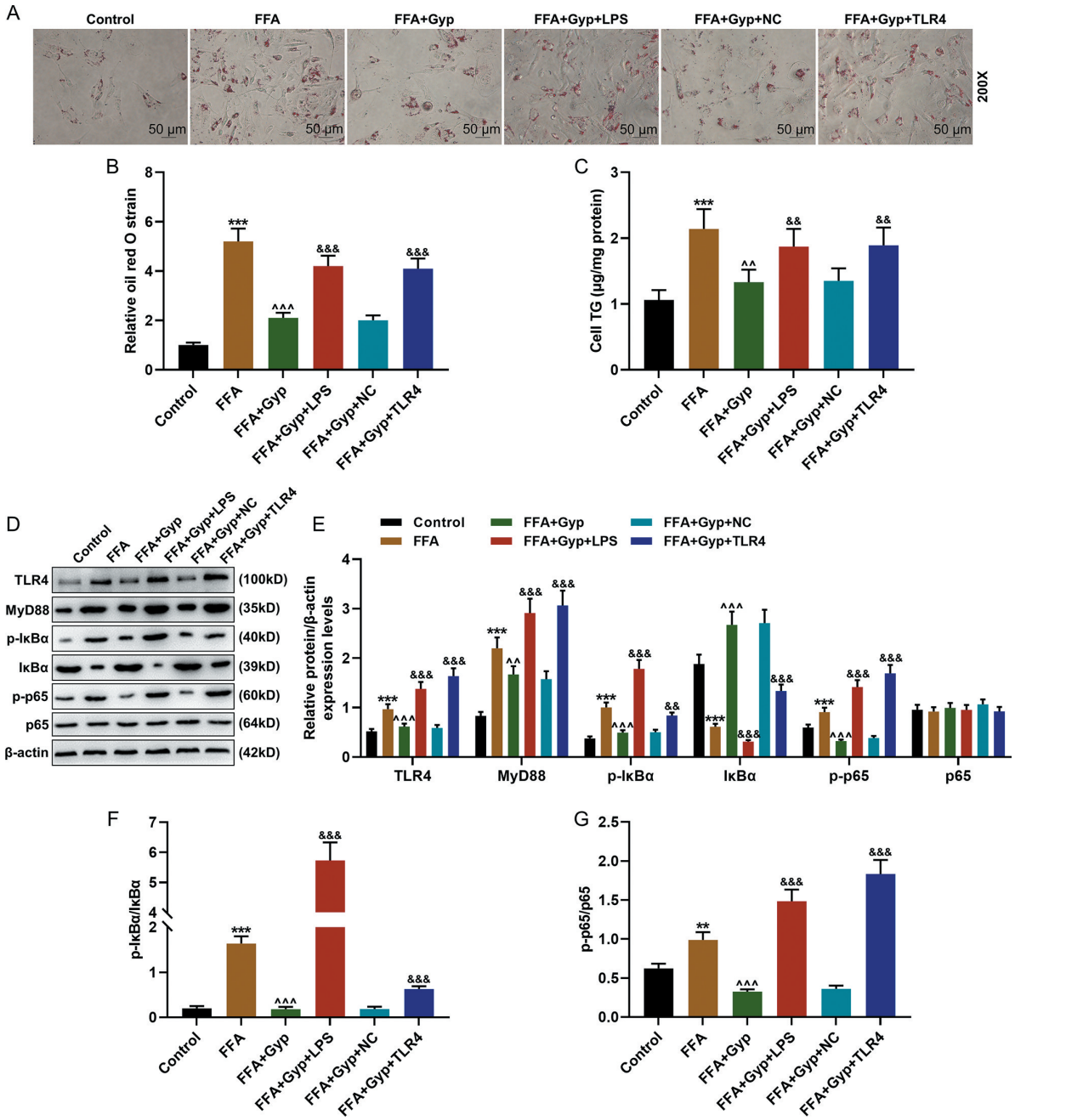

Figure 4. Effects of LPS stimulation or upregulating TLR4 signaling pathway on Gyp's inhibition of FFA-induced simple steatosis in THLE-2 cells. (a and b) Oil Red O staining was used to detect lipid droplet deposition. (c) Kit used to detect triglyceride (TG) content in cells. (D, E, F, and G) The expression levels of MyD88, p-IκBα, κBα, and p-p65 and p65 were detected by Western blotting. $n = 3$, $^{+}P < 0.05$, $^{++}P < 0.01$, $^{+++}P < 0.001$, vs. 0; $^{*}P < 0.05$, $^{**}P < 0.01$, $^{***}P < 0.001$, vs. Control; $^{\wedge}P < 0.05$, $^{\wedge\wedge}P < 0.01$, $^{\wedge\wedge\wedge}P < 0.001$, vs. FFA; $^{\#}P < 0.05$, $^{\#\#}P < 0.01$, $^{\#\#\#}P < 0.001$, vs. Gyp; $^{\&}P < 0.05$, $^{\&\&}P < 0.01$, $^{\&\&\&}P < 0.001$, vs. FFA+Gyp+NC.

nucleus. The results showed that the expression of p65 was decreased in the nucleus of FFA-induced cell model, and Gyp significantly reversed the FFA-induced decrease in p65. The results showed that the expression of p65 was increased in the nucleus of FFA-induced cell model, and Gyp significantly down-regulated the increase of p65 induced by FFA (Figure J-I, $P< 0.001$).

Effects of LPS stimulation or up-regulating TLR4 signaling pathway on Gypenosides-inhibited FFA-induced simple steatosis in THLE-2 cells

We further explored the effects of TLR4 signaling pathway on Gyp-inhibited FFA-induced simple steatosis in hepatocytes through cell experiments. The FFA-induced cells were treated with 50 ng/ml LPS and transfected with TLR4 overexpression vector. Oil Red O staining experiments showed that LPS stimulation and overexpressed TLR4 could inhibit lipid deposition in Gyp-treated high-fat model cells (Figure 4(a and b), $P< 0.001$). Moreover, the expression of TG was detected in THLE-2 cells, and the result showed that LPS stimulation and overexpressed TLR4 could significantly decrease the TG expression in Gyp-treated high-fat model cells (Figure 4(c), $P< 0.01$). Furthermore, the LPS/TLR4 pathway was detected by Western blotting, as shown in Figure 4(d-g), LPS stimulation and overexpressed TLR4 greatly reversed the effect of Gyp on decreasing the levels of TLR4, MyD88, p-IκBα, and p-p65 and increased IκBα level of FFA-induced cells ($P< 0.001$).

Discussion

Studies have found that Gyp can alleviate fatty liver infiltration in rats and reverse the fatty liver formation in a dose-dependent manner [18]. In this study we explored the effects of Gyp on blood lipids of the model rats fed with high-fat diet. Consistent with such results, we found that Gyp can protect fatty liver caused by high-fat diet.

Serum ALT and AST levels have been used as biochemical indicators for evaluating liver cell damage [21]. This study found that Gyp significantly reversed the AST and ALT levels increased by high-fat diet. At the same time, during lipid deposition oxidative stress can also cause damage to the mitochondrial membrane of hepatocytes, reduce the fluidity of the membrane, and release AST into the blood of mitochondria of hepatocytes, resulting in an increase in serum level of AST [22,23]. Therefore, in this study, we examined the changes in the levels of oxidative stress indicators MDA and SOD, and found that Gyp significantly increased SOD reduced by a high-fat diet and greatly reduced MDA increased by a high-fat diet.

Studies have suggested that NAFLD first induces lipid metabolism disorders and insulin resistance, leading to liver cell steatosis, and the inflammatory response progresses to the second stage, during which macrophages and neutrophils release inflammatory factors TNF-α, IL-1β, IL-6, etc., thereby aggravating liver cell damage and necrosis [24]. Previous studies showed that Gyp significantly reduces the levels of TNF-α and NF-κB and liver inflammation in fatty liver rats [25]; in addition, Kim's research showed that a high-fat diet can change the composition of intestinal bacteria, increase the serum concentration of LPS and mediate the inflammatory response via the TLR4 signaling pathway [26]. Therefore, we analyzed the effect of Gyp on the pathogenesis of NAFLD by detecting changes in the expression levels of inflammatory factors and TLR4 in model rats or cells. And we observed that Gyp significantly reduced the levels of inflammatory factors caused by high-fat diets.

Moreover, for blood lipids and insulin resistance, studies have found that Gyp can effectively reduce blood lipids and insulin levels in T2DM-NAFLD model rats [27]. In this study, we evaluated levels of HIS, FBG, and FINS in high-fat model rats. The results showed that Gyp significantly reduced the liver weight index, FBG, and FINS caused by a high-fat diet, which is consistent with the results of the study [28] (Table 2).

In order to reveal the mechanism of Gyp treatment in NAFLD rats, we explored whether Gyp improves the pathogenesis of NAFLD rats through the LPS/TLR4 signaling pathway. The study found that Gyp could reduce LPS-induced neuroinflammation, memory impairment and anxiety-like behaviors in rats, and can inhibit the increase of TLR4 levels in hippocampus in rats [29,30]. However, the role of its LPS/TLR4 signaling pathway in improving NAFLD was still unclear. Our study found that Gyp increased the expression of TLR4, LPS, MyD88, p-IκBα, and declined the expression of p-p65 and IκBα in NAFLD model.

The current increase in FFA is widely regarded as an important initiating factor for NAFLD [31]. Hepatocyte steatosis and liver

tissue inflammation are closely related to FFA changes [27]. Studies have shown that elevated FFA in either liver tissue or serum can cause a series of chain reactions: For example, liver cells take up FFA, which in turn increases TG synthesis and causes excessive accumulation of fat in the liver [32]. In this study, we used FFA to treat THLE-2 cells to establish a simple steatosis cell model. The Oil Red O staining showed that Gyp treatment can significantly reduce lipid droplet deposition in FFA-induced steatotic liver cells, and Gyp treatment can significantly reduce the increase in TG content in FFA-induced steatotic liver cells, and significantly down-regulate FFA-induced increases of levels of MyD88, p-IκBα, p-p65, and decrease of IκBα level due to up-regulation of high-fat diet. In addition, we further verified the effects of LPS stimulation or over-expression of TLR4-induced upregulation of TLR 4 signaling pathway on Gyp inhibition of FFA-induced simple steatosis in hepatocytes. The results showed that LPS stimulation or over-expression of TLR4 significantly reversed the effect of Gyp on improving FFA.

In conclusion, Gyp improves lipid metabolism and insulin resistance in nonalcoholic fatty liver rats by regulating LPS/TLR4 signaling pathway. LPS stimulation and overexpressed TLR4 could significantly reverse the effect of Gyp on reducing the levels of TLR4, MyD88, p-IκBα, and p-p65 and increasing IκBα level of FFA-induced cells. However, we also need to explore the effect of Gyp on FFA-induced cells by inhibiting the LPS/TLR4 signaling pathway from the opposite, for example, we will establish the silenced TLR4 vector transfect into FFA-induced hepatocytes. In addition, under FFA treatment, Gyp has more obvious effect on the pathway regulation, the specific reasons may require further research.

Acknowledgments

Not applicable.

Funding

This work was supported by the National Natural Science Foundation of China] under Grant [number 81503527]; China Postdoctoral Science Foundation under Grant [number 2016M601981]; the Science and Technology Planning Project of Traditional Chinese Medicine of Zhejiang Province, China [2017ZA045].

Data availability statement

The analyzed data sets generated during the study are available from the corresponding author on reasonable request.

Disclosure statement

No potential conflict of interest was reported by the authors.

Funding

This work was supported by the National Natural Science Foundation of China] under Grant [number 81503527]; China Postdoctoral Science Foundation under Grant [number 2016M601981]; the Science and Technology Planning Project of Traditional Chinese Medicine of Zhejiang Province, China [2017ZA045].

References

[1] Chakravarthy MV, Waddell T, Banerjee R, et al. Nutrition and nonalcoholic fatty liver disease: current perspectives. Gastroenterol Clin North Am. 2020;49(1):63–94.

[2] Ballestri S, Nascimbeni F, Baldelli E, et al. NAFLD as a sexual dimorphic disease: role of gender and reproductive status in the development and progression of nonalcoholic fatty liver disease and inherent cardiovascular risk. Adv Ther. 2017;34:1291–1326.

[3] Irvin MR, Zhi D, Joehanes R, et al. Epigenome-wide association study of fasting blood lipids in the genetics of lipid-lowering drugs and diet network study. Circulation. 2014;130(7):565–572. .

[4] Tang XR, Wang JX, Fu L, et al. Effects of total flavonoids in astragali complanati semen on liver lipid level and ERalpha expression on liver in hyperlipidemia rats with kidney-Yang deficiency pattern. Zhongguo Zhong Yao Za Zhi. 2018;43:2365–2371.

[5] Kiziltas S, Ata P, Colak Y, et al. TLR4 gene polymorphism in patients with nonalcoholic fatty liver disease in comparison to healthy controls. Metab Syndr Relat Disord. 2014;12(3):165–170.

[6] Miura K, Ohnishi H. Role of gut microbiota and Toll-like receptors in nonalcoholic fatty liver disease. World J Gastroenterol. 2014;20(23):7381–7391.

[7] Roh YS, Seki E. Toll-like receptors in alcoholic liver disease, non-alcoholic steatohepatitis and carcinogenesis. J Gastroenterol Hepatol. 2013;28 (Suppl 1):38–42.

[8] Yuan Y, Gong X, Zhang L, et al. Chlorogenic acid ameliorated concanavalin A-induced hepatitis by suppression of Toll-like receptor 4 signaling in mice. Int Immunopharmacol. 2017;44:97–104.
[9] Zhang J, Tan YQ, Wei MH, et al. TLR4-induced B7-H1 on keratinocytes negatively regulates CD4+T cells and CD8+T cells responses in oral lichen planus. Exp Dermatol. 2017;26(5):409–415.
[10] Plociennikowska A, Hromada-Judycka A, Borzecka K, et al. Co-operation of TLR4 and raft proteins in LPS-induced pro-inflammatory signaling. Cell Mol Life Sci. 2015;72:557–581.
[11] Xu Y, Yang C, Zhang S, et al. Ginsenoside Rg1 protects against non-alcoholic fatty liver disease by ameliorating lipid peroxidation, endoplasmic reticulum stress, and inflammasome activation. Biol Pharm Bull. 2018;41 (11):1638–1644.
[12] Nier A, Huber Y, Labenz C, et al. Adipokines and endotoxemia correlate with hepatic steatosis in non-alcoholic fatty liver disease (NAFLD). Nutrients. 2020;12(3):699.
[13] Rossato M, Di Vincenzo A, Pagano C, et al. The P2X7 receptor and NLRP3 axis in non-alcoholic fatty liver disease: a brief review. Cells. 2020;9(4):1047.
[14] Belegri E, Eggels L, la Fleur SE, et al. One-week exposure to a free-choice high-fat high-sugar diet does not interfere with the lipopolysaccharide-induced acute phase response in the hypothalamus of male rats. Front Endocrinol (Lausanne). 2018;9:186.
[15] Ding PH, Darveau RP, Wang CY, et al. 3LPS-binding protein and its interactions with P. gingivalis LPS modulate pro-inflammatory response and Toll-like receptor signaling in human oral keratinocytes. PloS One. 2017;12(4):e0173223.
[16] Liu Q, Zhu L, Cheng C, et al. Natural active compounds from plant food and Chinese herbal medicine for nonalcoholic fatty liver disease. Curr Pharm Des. 2017;23:5136–5162.
[17] Kong L, Wang X, Zhang K, et al. Gypenosides synergistically enhances the anti-tumor effect of 5-fluorouracil on colorectal cancer in vitro and in vivo: a role for oxidative stress-mediated DNA damage and p53 activation. PloS One. 2015;10(9):e0137888.
[18] Gou SH, Huang HF, Chen XY, et al. Lipid-lowering, hepatoprotective, and atheroprotective effects of the mixture Hong-Qu and gypenosides in hyperlipidemia with NAFLD rats. J Chin Med Assoc. 2016;79(3):111–121.
[19] Livak KJ, Schmittgen TD. Analysis of relative gene expression data using real-time quantitative PCR and the 2(-Delta Delta C(T)) method. Methods. 2001;25 (4):402–408.
[20] Chen Z, Xu YY, Wu R, et al. Impaired learning and memory in rats induced by a high-fat diet: involvement with the imbalance of nesfatin-1 abundance and copine 6 expression. J Neuroendocrinol. 2017;29(4). DOI:10.1111/jne.12462
[21] Liu Y, Yang X, Jing Y, *et al*. Contribution and mobilization of mesenchymal stem cells in a mouse model of carbon tetrachloride-induced liver fibrosis. Sci Rep. 2015;5(1):17762. .
[22] Alshammari GM, Balakrishnan A, Chinnasamy T. Nimbolide attenuate the lipid accumulation, oxidative stress and antioxidant in primary hepatocytes. Mol Biol Rep. 2017;44(6):463–474.
[23] Elgebaly HA, Mosa NM, Allach M, et al. Olive oil and leaf extract prevent fluoxetine-induced hepatotoxicity by attenuating oxidative stress, inflammation and apoptosis. Biomed Pharmacothe. 2018;98:446–453.
[24] Ma C, Kesarwala AH, Eggert T, *et al*. NAFLD causes selective CD4+ T lymphocyte loss and promotes hepatocarcinogenesis. Nature. 2016;531 (7593):253–257. .
[25] Henao-Mejia J, Elinav E, Jin C, *et al*. Inflammasome-mediated dysbiosis regulates progression of NAFLD and obesity. Nature. 2012;482(7384):179–185. .
[26] Kim KA, Gu W, Lee IA, et al. High fat diet-induced gut microbiota exacerbates inflammation and obesity in mice via the TLR4 signaling pathway. PloS One. 2012;7(10):e47713.
[27] Zhang XQ, Pan Y, Yu CH, et al. PDIA3 knockdown exacerbates free fatty acid-induced hepatocyte steatosis and apoptosis. PloS One. 2015;10(7):e0133882.
[28] He Q, Li JK, Li F, et al. Mechanism of action of gypenosides on type 2 diabetes and non-alcoholic fatty liver disease in rats. World J Gastroenterol. 2015;21 (7):2058–2066.
[29] Lee B, Shim I, Lee H. Gypenosides attenuate lipopolysaccharide-induced neuroinflammation and memory impairment in rats. Evid Based Complement Alternat Med. 2018;2018:4183670.
[30] Lee B, Shim I, Lee H, et al. Gypenosides attenuate lipopolysaccharide-induced neuroinflammation and anxiety-like behaviors in rats. Animal cells Sys. 2018;22 (5):305–316. .
[31] Chen Q, Liu M, Yu H, et al. Scutellaria baicalensis regulates FFA metabolism to ameliorate NAFLD through the AMPK-mediated SREBP signaling pathway. J Nat Med. 2018;72:655–666.
[32] Liu YL, Lin LC, Tung YT, et al. Rhododendron oldhamii leaf extract improves fatty liver syndrome by increasing lipid oxidation and decreasing the lipogenesis pathway in mice. Int J Med Sci. 2017;14 (9):862–870.